Numerical Formulations and Applications of the ADI-FDTD Method

Takefumi Namiki

Computational Science and Engineering Center, Fujitsu Limited
9-3, Nakase 1-Chome, Mihama-ku, Chiba City, Chiba 261-8588, Japan
TEL:+81-43-299-3240, FAX:+81-43-299-3010, email: t.namiki@jp.fujitsu.com

Abstract – In this paper, the ADI-FDTD (Alternating-Direction-Implicit Finite-Difference Time-Domain) method is presented. As the algorithm of the method is unconditionally stable and free from the Courant-Friedrich-Levy (CFL) stability condition restraint, a time-step size larger than the CFL limit can be set and computation time can be saved for some problems. Numerical formulations are explained and simulation results are compared with those of the conventional FDTD method.

1. Introduction

The finite-difference time-domain (FDTD) method [1][2] has been applied to various problems related to electromagnetism. As the traditional FDTD method is based on an explicit finite difference algorithm, the numerical formulations are quit simple and its computation is very efficient. However, the Courant-Friedrich-Levy (CFL) stability condition must be satisfied when this method is used. Therefore, the maximum time-step size is limited by minimum cell size in the computational domain. As a result, if an object of analysis has fine scale dimensions compared with wavelength, the small time-step size creates a significant increase in calculation time.

To eliminate the CFL stability condition, applying implicit techniques to the FDTD scheme is required. In 1984, Holland reported an implicit FDTD method [3] but it was not completely stable. There have been few works on the implicit approaches since. Thus, no one had succeeded in constructing unconditionally stable FDTD schemes until 1998. We first reported the unconditionally stable FDTD method in two- and three-dimensions [4][5] in 1998. Because they are based on the alternating-direction-implicit (ADI) method [6], we called them the ADI-FDTD method. Our approaches were also published in IEEE transactions [7][8]. Soon after having published our findings, Zheng et al. reported the same approach [9] and theoretically proved the stability of the scheme in three-dimensions [10].

The ADI method is known as the implicit finite-difference algorithm, which has the advantage of ensuring a more efficient formulation and calculation than other implicit methods in the case of multidimensional problems. The ADI method has been widely applied to parabolic equations for solving heat transfer problems [6].

In this paper, numerical formulations of the ADI-FDTD method are explained and simulation results are compared with those of the conventional FDTD method.

2. Numerical Formulations

2.1 Fundamental Equations [8]

The numerical formulations of the ADI-FDTD method for a full three-dimensional wave are presented in (1)-(12). The electromagnetic field components are arranged on the cells in the same manner as the conventional FDTD method. These formulations are applicable to inhomogeneous lossy medium as well as to nonuniform cells. The calculation for one discrete time step is performed using two procedures. The first procedure is based on (1)-(6) and the second procedure is based on (7)-(12) as follows:

<First procedure>

$$E_{x(i+1/2,j,k)}^{n+1/2} = C_{a(i+1/2,j,k)} \cdot E_{x(i+1/2,j,k)}^{n} + C_{b(i+1/2,j,k)} \cdot \left[\{ H_{z(i+1/2,j+1/2,k)}^{n} - H_{z(i+1/2,j-1/2,k)}^{n} \} / \Delta y(j) - \{ H_{y(i+1/2,j,k+1/2)}^{n+1/2} - H_{y(i+1/2,j,k-1/2)}^{n+1/2} \} / \Delta z(k) \right] \quad (1)$$

$$E_{y(i,j+1/2,k)}^{n+1/2} = C_{a(i,j+1/2,k)} \cdot E_{y(i,j+1/2,k)}^{n} + C_{b(i,j+1/2,k)} \cdot \left[\{ H_{x(i,j+1/2,k+1/2)}^{n} - H_{x(i,j+1/2,k-1/2)}^{n} \} / \Delta z(k) - \{ H_{z(i+1/2,j+1/2,k)}^{n+1/2} - H_{z(i-1/2,j+1/2,k)}^{n+1/2} \} / \Delta x(i) \right] \quad (2)$$

$$E_{z(i,j,k+1/2)}^{n+1/2} = C_{a(i,j,k+1/2)} \cdot E_{z(i,j,k+1/2)}^{n} + C_{b(i,j,k+1/2)} \cdot \left[\{ H_{y(i+1/2,j,k+1/2)}^{n} - H_{y(i-1/2,j,k+1/2)}^{n} \} / \Delta x(i) - \{ H_{x(i,j+1/2,k+1/2)}^{n+1/2} - H_{x(i,j-1/2,k+1/2)}^{n+1/2} \} / \Delta y(j) \right] \quad (3)$$

$$H_{x(i,j+1/2,k+1/2)}^{n+1/2} = H_{x(i,j+1/2,k+1/2)}^{n} + D_{b(i,j+1/2,k+1/2)} \cdot \left[\{ E_{y(i,j+1/2,k+1)}^{n} - E_{y(i,j+1/2,k)}^{n} \} / \Delta z(k) - \{ E_{z(i,j+1,k+1/2)}^{n+1/2} - E_{z(i,j,k+1/2)}^{n+1/2} \} / \Delta y(j) \right] \quad (4)$$

$$H_{y(i+1/2,j,k+1/2)}^{n+1/2} = H_{y(i+1/2,j,k+1/2)}^{n} + D_{b(i+1/2,j,k+1/2)} \cdot \left[\{ E_{z(i+1,j,k+1/2)}^{n} - E_{z(i,j,k+1/2)}^{n} \} / \Delta x(i) - \{ E_{x(i+1/2,j,k+1)}^{n+1/2} - E_{x(i+1/2,j,k)}^{n+1/2} \} / \Delta z(k) \right] \quad (5)$$

$$H_{z(i+1/2,j+1/2,k)}^{n+1/2} = H_{z(i+1/2,j+1/2,k)}^{n} + D_{b(i+1/2,j+1/2,k)} \cdot \left[\{ E_{x(i+1/2,j+1,k)}^{n} - E_{x(i+1/2,j,k)}^{n} \} / \Delta y(j) - \{ E_{y(i+1,j+1/2,k)}^{n+1/2} - E_{y(i,j+1/2,k)}^{n+1/2} \} / \Delta x(i) \right] \quad (6)$$

<Second procedure>

$$E_{x(i+1/2,j,k)}^{n+1} = C_{a(i+1/2,j,k)} \cdot E_{x(i+1/2,j,k)}^{n+1/2} + C_{b(i+1/2,j,k)} \cdot \left[\{ H_{z(i+1/2,j+1/2,k)}^{n+1} - H_{z(i+1/2,j-1/2,k)}^{n+1} \} / \Delta y(j) - \{ H_{y(i+1/2,j,k+1/2)}^{n+1/2} - H_{y(i+1/2,j,k-1/2)}^{n+1/2} \} / \Delta z(k) \right] \quad (7)$$

$$E_{y(i,j+1/2,k)}^{n+1} = C_{a(i,j+1/2,k)} \cdot E_{y(i,j+1/2,k)}^{n+1/2} + C_{b(i,j+1/2,k)} \cdot \left[\{ H_{x(i,j+1/2,k+1/2)}^{n+1} - H_{x(i,j+1/2,k-1/2)}^{n+1} \} / \Delta z(k) - \{ H_{z(i+1/2,j+1/2,k)}^{n+1/2} - H_{z(i-1/2,j+1/2,k)}^{n+1/2} \} / \Delta x(i) \right] \quad (8)$$

$$E_{z(i,j,k+1/2)}^{n+1} = C_{a(i,j,k+1/2)} \cdot E_{z(i,j,k+1/2)}^{n+1/2} + C_{b(i,j,k+1/2)} \cdot \left[\{ H_{y(i+1/2,j,k+1/2)}^{n+1} - H_{y(i-1/2,j,k+1/2)}^{n+1} \} / \Delta x(i) - \{ H_{x(i,j+1/2,k+1/2)}^{n+1/2} - H_{x(i,j-1/2,k+1/2)}^{n+1/2} \} / \Delta y(j) \right] \quad (9)$$

$$H_{x(i,j+1/2,k+1/2)}^{n+1} = H_{x(i,j+1/2,k+1/2)}^{n+1/2} + D_{b(i,j+1/2,k+1/2)} \cdot \left[\{ E_{y(i,j+1/2,k+1)}^{n+1} - E_{y(i,j+1/2,k)}^{n+1} \} / \Delta z(k) - \{ E_{z(i,j+1,k+1/2)}^{n+1/2} - E_{z(i,j,k+1/2)}^{n+1/2} \} / \Delta y(j) \right] \quad (10)$$

$$H_{y(i+1/2,j,k+1/2)}^{n+1} = H_{y(i+1/2,j,k+1/2)}^{n+1/2} + D_{b(i+1/2,j,k+1/2)} \cdot \left[\{ E_{z(i+1,j,k+1/2)}^{n+1} - E_{z(i,j,k+1/2)}^{n+1} \} / \Delta x(i) - \{ E_{x(i+1/2,j,k+1)}^{n+1/2} - E_{x(i+1/2,j,k)}^{n+1/2} \} / \Delta z(k) \right] \quad (11)$$

$$H_{z(i+1/2,j+1/2,k)}^{n+1} = H_{z(i+1/2,j+1/2,k)}^{n+1/2} + D_{b(i+1/2,j+1/2,k)} \cdot \left[\{ E_{x(i+1/2,j+1,k)}^{n+1} - E_{x(i+1/2,j,k)}^{n+1} \} / \Delta y(j) - \{ E_{y(i+1,j+1/2,k)}^{n+1/2} - E_{y(i,j+1/2,k)}^{n+1/2} \} / \Delta x(i) \right] \quad (12)$$

The coefficients are defined in the same manner as the conventional FDTD method and they are as follows:

$$C_a(i,j,k) = \frac{2\varepsilon(i,j,k)-\sigma(i,j,k)\Delta t}{2\varepsilon(i,j,k)+\sigma(i,j,k)\Delta t}$$

$$C_b(i,j,k) = \frac{2\Delta t}{2\varepsilon(i,j,k)+\sigma(i,j,k)\Delta t}$$

$$D_b(i,j,k) = \frac{\Delta t}{\mu(i,j,k)}$$

2.2 Tridiagonal Systems of Equations

Equations (1)-(12) can not be applied directly for numerical calculation because they include the components defined as synchronous variables on both the left- and right-hand side, so modified equations are derived from the original equations.

In the first procedure, the E_x component on the left-hand side and the H_y components on the right-hand side are defined as synchronous variables in (1), thus, a modified (1') for the E_x component is derived from (1) and (5) by eliminating the $H_y^{n+1/2}$ components. The suffix k in (1') spans all values in z and indicates the maximum number of simultaneous linear equations which are involved in the implicit update of E_x. This is called the z-directional scan of E_x.

$$-\alpha_1 E_{x(i+1/2,j,k-1)}^{n+1/2} + \beta_1 E_{x(i+1/2,j,k)}^{n+1/2} - \gamma_1 E_{x(i+1/2,j,k+1)}^{n+1/2} = \mathrm{T1}_{(i,j,k)}^{n} \qquad (1')$$

where

$$\alpha_1 = D_{b(i+1/2,j,k-1/2)} / \Delta z(k)^2$$

$$\beta_1 = 1 / C_{b(i+1/2,j,k)} + \alpha_1 + \gamma_1$$

$$\gamma_1 = D_{b(i+1/2,j,k+1/2)} / \Delta z(k)^2$$

$$\begin{aligned}\mathrm{T1}_{(i,j,k)}^{n} = {} & p_1 E_{x(i+1/2,j,k)}^{n} \\ & + \{H_{z(i+1/2,j+1/2,k)}^{n} - H_{z(i+1/2,j-1/2,k)}^{n}\} / \Delta y(j) \\ & - \{H_{y(i+1/2,j,k+1/2)}^{n} - H_{y(i+1/2,j,k-1/2)}^{n}\} / \Delta z(k) \\ & + q_1 \{E_{z(i+1,j,k-1/2)}^{n} - E_{z(i,j,k-1/2)}^{n}\} / \{\Delta x(i) \Delta z(k)\} \\ & - r_1 \{E_{z(i+1,j,k+1/2)}^{n} - E_{z(i,j,k+1/2)}^{n}\} / \{\Delta x(i) \Delta z(k)\}\end{aligned}$$

$$p_1 = C_{a(i+1/2,j,k)} / C_{b(i+1/2,j,k)}$$

$$q_1 = D_{b(i+1/2,j,k-1/2)}$$

$$r_1 = D_{b(i+1/2,j,k+1/2)}$$

In the same way, the implicit equations for the $E_y^{n+1/2}$ and $E_z^{n+1/2}$ components are derived from (2), (6) and (3), (4), respectively. These update expressions involved all index value of x and y, respectively. By solving these simultaneous linear equations, we can get the values of the electric field components at the time of n+1/2. Thereafter, we can get the values of the magnetic field components at the time of n+1/2 directly by (4)-(6).

In the second procedure, the E_x component on the left-hand side and the H_z components on the right-hand side are defined as synchronous variables in (7), thus, a modified (7') for the E_x component is derived from (7) and (12) by eliminating the H_z^{n+1} components. The suffix j in (7') spans all values in y and indicates the maximum number of simultaneous linear equations which are involved in the implicit update of E_x. This is called the y-directional scan of E_x.

$$-\alpha_2 E_{x(i+1/2,j-1,k)}^{n+1} + \beta_2 E_{x(i+1/2,j,k)}^{n+1} - \gamma_2 E_{x(i+1/2,j+1,k)}^{n+1} = \mathrm{T2}_{(i,j,k)}^{n+1/2} \qquad (7')$$

where

$$\alpha_2 = D_{b(i+1/2,j-1/2,k)} / \Delta y(j)^2$$

$$\beta_2 = 1 / C_{b(i+1/2,j,k)} + \alpha_2 + \gamma_2$$

$$\gamma_2 = D_{b(i+1/2,j+1/2,k)} / \Delta y(j)^2$$

$$\begin{aligned}\mathrm{T2}_{(i,j,k)}^{n+1/2} = {} & p_2 E_{x(i+1/2,j,k)}^{n+1/2} \\ & + \{H_{z(i+1/2,j+1/2,k)}^{n+1/2} - H_{z(i+1/2,j-1/2,k)}^{n+1/2}\} / \Delta y(j) \\ & - \{H_{y(i+1/2,j,k+1/2)}^{n+1/2} - H_{y(i+1/2,j,k-1/2)}^{n+1/2}\} / \Delta z(k) \\ & + q_2 \{E_{y(i+1,j-1/2,k)}^{n+1/2} - E_{y(i,j-1/2,k)}^{n+1/2}\} / \{\Delta x(i) \Delta y(j)\} \\ & - r_2 \{E_{y(i+1,j+1/2,k)}^{n+1/2} - E_{y(i,j+1/2,k)}^{n+1/2}\} / \{\Delta x(i) \Delta y(j)\}\end{aligned}$$

$$p_2 = C_{a(i+1/2,j,k)} / C_{b(i+1/2,j,k)}$$

$$q_2 = D_{b(i+1/2,j-1/2,k)}$$

$$r_2 = D_{b(i+1/2,j+1/2,k)}$$

In the same way, the implicit equations for the E_y^{n+1} and E_z^{n+1} components are derived from (8), (10) and (9), (11), respectively. These update expressions involved all index value of z and x, respectively. By solving these simultaneous linear equations, we can get the values of the electric field components at the

time of $n+1$. Thereafter, we can get the values of the magnetic field components at the time of $n+1$ directly by (10)-(12).

The simultaneous equations can be written in tridiagonal matrix form and (1') is expressed as follows:

$$\begin{pmatrix} \beta_{(1)} & \gamma_{(1)} & & & 0 \\ \alpha_{(2)} & \beta_{(2)} & \gamma_{(2)} & & \\ & \ddots & & & \\ & & \alpha_{(nk-1)} & \beta_{(nk-1)} & \gamma_{(nk-1)} \\ 0 & & & \alpha_{(nk)} & \beta_{(nk)} \end{pmatrix} \begin{pmatrix} E_{x(1)}^{n+1/2} \\ E_{x(2)} \\ \vdots \\ E_{x(nk-1)} \\ E_{x(nk)} \end{pmatrix} = \begin{pmatrix} \mathrm{T}_{(1)}^{n} \\ \mathrm{T}_{(2)} \\ \vdots \\ \mathrm{T}_{(nk-1)} \\ \mathrm{T}_{(nk)} \end{pmatrix} \quad (1'')$$

For the tridiagonal systems of equations, the procedures of LU decomposition, forward- and backward-substitution each take only $O(N)$ operations, and the whole solution can be encoded very concisely [11].

2.3 Treatment of Boundary Conditions

In the case of the ADI-FDTD method, we must add special treatment in the matrix form for the boundary conditions of the electric-field components. The first and last rows in (1") indicate formulations for calculating the E_x components at the z-directional terminals. Absorbing boundary conditions (ABCs) are commonly set on the outer surfaces of the computational domain, so they must be formulated in the rows. For the implementation, ABCs based on the one-way wave equation is applied. Mur's first-order ABC [12] is as follows:

$$E_{x(k=1)}^{n+1/2} - E_{x(k=2)}^{n} = s\left[E_{x(k=2)}^{n+1/2} - E_{x(k=1)}^{n}\right]$$

$$E_{x(k=kn)}^{n+1/2} - E_{x(k=kn-1)}^{n} = s\left[E_{x(k=kn-1)}^{n+1/2} - E_{x(k=kn)}^{n}\right]$$

where

$$s = \frac{c(\Delta t/2) - \Delta z}{c(\Delta t/2) + \Delta z}$$

By applying them into (1"), we have

$$\beta_{(1)} = 1.0, \quad \gamma_{(1)} = -s, \quad \mathrm{T}_{(1)}^{n} = E_{x(2)}^{n} - sE_{x(1)}^{n}$$

$$\beta_{(nk)} = 1.0, \quad \alpha_{(nk)} = -s, \quad \mathrm{T}_{(nk)}^{n} = E_{x(nk-1)}^{n} - sE_{x(nk)}^{n}$$

In the first procedure, E_x components at the y-directional terminals are calculated in the same way as the conventional method. Other ABCs are also applicable to the ADI-FDTD method. In fact, Bererenger's PML [13] has successfully been applied to this scheme [14][15].

Perfect electric conductor (PEC) boundary conditions are also often used in the FDTD method. At the surface of the PEC, tangential electric field must be zero. For example, if the condition

$$E_{x(k)}^{n} = 0$$

is required, the following must be held:

$$\alpha_{(k)} = 0, \quad \beta_{(k)} = 1, \quad \gamma_{(k)} = 0, \quad \mathrm{T}_{(k)}^{n} = 0$$

Source conditions are applied similarly. If the hard-source excitation

$$E_{x(k)}^{n+1/2} = E_0 \sin[2\pi f_0 (n+1/2)\Delta t]$$

is required, the following must be set:

$$\alpha_{(k)} = 0, \beta_{(k)} = 1, \gamma_{(k)} = 0, \mathrm{T}_{(k)}^{n} = \sin[2\pi f_0 (n+1/2)\Delta t]$$

However, the soft-source excitation is performed in a different way [16].

As mentioned above, the implicit formulation should be used to implement boundary conditions of the electric fields.

3. Numerical Examples

3.1 Microstrip Linear Resonator [17]

Fig.1 shows the horizontal structure of the microstrip linear resonator and it is characterized as follows. The substrate is 810 μm thick with relative permittivity of 3.25. The width and thickness of the strip is 1.842 mm and 18 μm, respectively, thereby rendering the thickness negligible for numerical modeling. There are two gaps with widths of 80 μm. The length of the internal strip is 22 mm. We use nonuniform cells in order to treat the narrow gaps and the long microstrip lines. The spatial modeling is shown in detail in fig.2. The substrate region is divided into 6 cells in the x-direction and the strip region is divided into 12 cells in the y-direction. The 80-μm-wide gap region is divided into 4 cells in the z-direction, in which the minimum cells, which are $153.5 \times 135 \times 20\ \mu m^3$, are placed. The CFL stability condition of this model is derived from the minimum cells and is $\Delta t \leq 65.4059$ fs. The total

number of cells is 22 × 44 × 78 = 75504. PEC boundary conditions are applied at the strips and at the ground plane. Mur's first-order ABCs are applied on all outer surfaces except the bottom ground plane. A Gaussian pulse is excited at one terminal and the output voltage is observed at the other terminal. By applying a Fourier transformation to the incident and output pulses, the insertion loss of the resonator can be calculated.

The time-step size for the conventional FDTD method is set so as to satisfy the CFL stability condition, and the time-step size for the ADI-FDTD method is set to 5, 10, or 20 times as large as the previous size. A physical time of each simulation is required about 12 ns for the oscillation of the output pulse to converge.

The calculated and measured insertion losses of the resonator are shown in fig.3. The time-step size and the required CPU time for each calculation are shown in table 1. The required memory size for the ADI-FDTD method is about 1.9 times as large as that for the conventional FDTD method because of the necessity of using extra electromagnetic component and coefficient array storage, which is common to all examples. The calculated insertion loss of the FDTD is quite similar to the measured data although the level of the FDTD is a little high and its response is shifted downward slightly in terms of frequency. Comparing the results of the ADI-FDTD method with those of the conventional FDTD method, we can see that there are differences depending on the time-step size. The resonant frequencies extracted from the insertion losses are shown in table 2, which also shows the relative errors of the calculated results with respect to the measured data. It can be seen, quantitatively, that the increase in time-step size resulted in a reduction of the resonant frequency.

As mentioned above, the tradeoff resulting from an increase in time-step size, which effects a reduction in CPU time, is an increase in numerical errors. This is a sample indicating that the ADI-FDTD method can be as accurate and efficient as the conventional FDTD method. However, the ADI-FDTD method will have an advantage over the conventional FDTD method if a similar model includes smaller minimum cells in the computational domain.

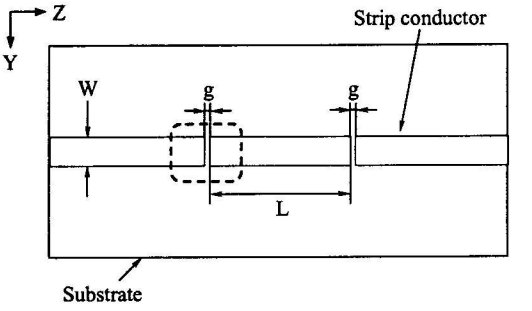

Fig. 1. Microstrip linear resonator (horizontal plane).

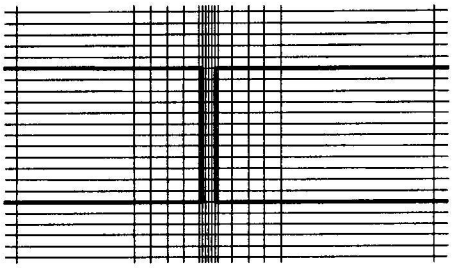

Fig. 2. Spatial discretization around the gap.

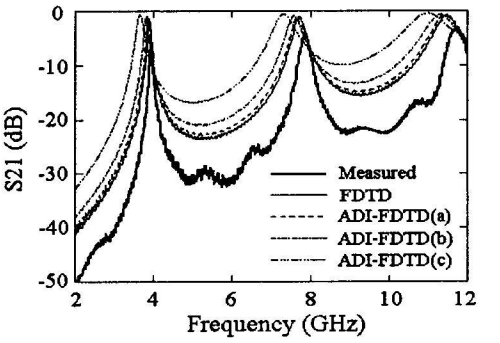

Fig. 3. Insertion loss of the microstrip linear resonator.

Table 1 Time-step size and CPU time

	Time-step size		CPU time	
	fs	ratio	min	ratio
FDTD	65.0	1.0	68.1	1.00
ADI-FDTD (a)	325.0	5.0	72.7	1.07
ADI-FDTD (b)	650.0	10.0	33.4	0.49
ADI-FDTD (c)	1300.0	20.0	16.8	0.25

Table 2 Resonant frequencies

	First mode		Second mode		Third mode	
	Resonant frequency	Relative error	Resonant frequency	Relative error	Resonant frequency	Relative error
Measured	3.95GHz	——	7.85GHz	——	11.76GHz	——
FDTD	3.90GHz	1.3%	7.72GHz	1.7%	11.48GHz	2.4%
ADI-FDTD (a)	3.87GHz	2.0%	7.68GHz	2.2%	11.46GHz	2.6%
ADI-FDTD (b)	3.83GHz	3.0%	7.58GHz	3.4%	11.31GHz	3.8%
ADI-FDTD (c)	3.66GHz	7.3%	7.32GHz	6.8%	10.99GHz	6.5%

3.2 Thin Conductive Enclosure [18]

Figs.4 and 5 show a model for estimating shielding effectiveness (SE). It consists of a half-cubic conductive shell on a ground plane. The shell is 56 × 56 × 25 mm^3 and is composed of 24-μm-thick conductive material with relative permittivity of 1.0, relative permeability of 1.0, and conductivity of 2400 S/m. Nonuniform cells are used to treat both the thin sheets of the shell and a wide computational region. A partial Gaussian pulse is applied at the excitation point, and the field at the observation point is output. Numerical calculations are carried out two times, with and without the shell. The SE values are calculated by applying a Fourier transformation to each output field. To estimate the electric field SE, vertical electric field components are used. Mur's ABCs are applied at all outer surfaces of the computational domain except the bottom ground plane. The SE values are calculated for the shell using the ADI-FDTD method and the conventional FDTD method. These results are compared with experimental data and analytical solutions.

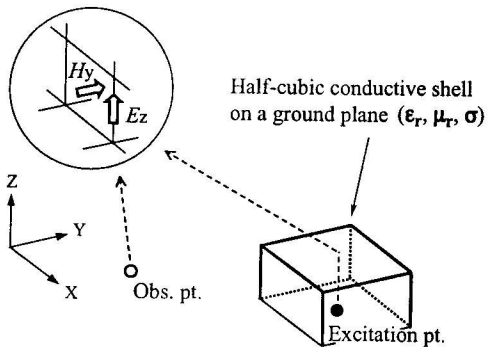

Fig. 4. Half-cubic conductive shell on a ground plane.

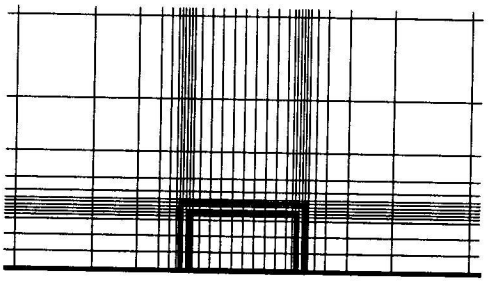

Fig. 5. Spatial discretization of the shell model.

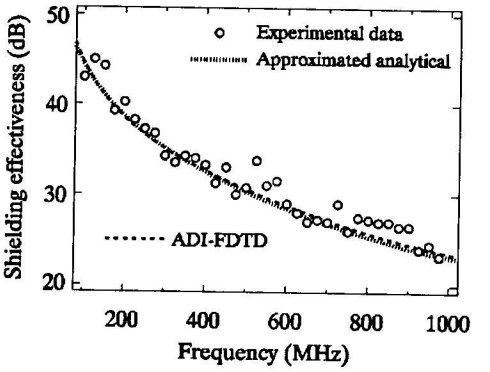

Fig. 6. Shielding effectiveness for electric field.

Fig.6 shows the SE values for fields for the shell. The numerical results for the ADI-FDTD method and the approximated analytical solution agree quite well. Moreover, they are quite similar to the experimental data.

There are no results for the conventional FDTD method here due to the extreme computational costs. Although numerical results cannot be obtained by the conventional FDTD method, table 3 lists the estimated computational effort for the two methods. The time-step size for the ADI-FDTD method is set 62 times larger than that for the conventional FDTD method. Consequently, the required CPU time for the ADI-FDTD method is reduced to 6.2% of that for the conventional FDTD method.

Table 3 Time-step size and CPU time

	Time-step size		CPU time	
	fs	ratio	s	ratio
FDTD	15.38	1.0	60060	1.0
ADI-FDTD	960.0	62.4	3749	0.062

4. Conclusion

The ADI-FDTD method is unconditionally stable, so the limitation of the maximum time-step size does not depend on the CFL stability condition but rather on numerical errors. The tradeoff resulting from an increase in time-step size, which effects a reduction in CPU time, is an increase in numerical errors. What limits the maximum time-step size depends on what kinds of problems or models are calculated. There is no guideline to decide a most appropriate time-step size for a problem. However, if the size of the local minimum cell in the computational domain is much smaller than the wavelength, the error limitation of the time-step size may be larger than the CFL limitation. In this case, the ADI-FDTD method is more efficient than the conventional FDTD method.

We have two subsequent works on the ADI-FDTD method. One is applying the method to many kinds of realistic problem and finding numerical models in which the method has the advantages compared with the conventional FDTD method. The other is developing advanced techniques on the method to improve the calculation accuracy when a large time-step size is used.

Acknowledgment

The author would like to thank Dr. J. Alan Roden, IBM Microelectronics, USA, for his usefull suggestions and great help to publish this article.

References

[1] K. S. Yee, "Numerical solution of initial boundary value problems involving Maxwell's equations in isotropic media," IEEE Trans. Antennas and Propagation, vol. AP-14, pp. 302-307, May 1966.

[2] A. Taflove, *Computational electrodynamics*. Norwood, MA: Artech House, 1995

[3] R. Holland, "Implicit three-dimensional finite differencing of Maxwell's equations," IEEE Trans. Nucl. Sci., vol. NS-31, pp. 1322-1326, 1984.

[4] T. Namiki and K.Ito, "Fundamental study of alternating direction implicit FDTD method for two dimensional problems," Technical Report of IEICE, AP98-21, pp. 31-37, June 1998.

[5] T. Namiki and K.Ito, "A study of numerical simulation of transmission line using ADI-FDTD method," Technical Report of IEICE, MW98-83, pp. 57-63, Sep. 1998.

[6] G.D. Smith, *Numerical solution of partial differential equations*. Oxford, U.K.: Oxford University Press, 1965.

[7] T. Namiki, "A new FDTD algorithm based on alternating direction implicit method," IEEE Trans. Microwave Theory Tech., vol. MTT-47, No. 10, pp. 2003-2007 Oct. 1999.

[8] T. Namiki, "3-D ADI-FDTD method – Unconditionally Stable Time-Domain Algorithm for Solving Full Vector Maxwell's Equations," IEEE Trans. Microwave Theory Tech., vol. MTT-48, no. 10, pp. 1743-1748, Oct. 2000.

[9] F.Zheng, Z.Chen, and J.Zhang, "A finite-Difference Time-Domain Method without the Courant Stability Condition," IEEE Microwave and Guided Wave Letters, vol. 9, no. 11, pp. 441-443, Nov. 1999.

[10] F. Zheng, Z. Chen, and J. Zhang, "Toward the Development of a Three-Dimensional Unconditionally Stable Finite-Difference Time-Domain Method," IEEE Trans. Microwave Theory Tech., vol. MTT-48, no. 9, pp. 1550-1558, Sep. 2000.

[11] W. H. Press et al., *Numerical recipes in FORTRAN*, 2nd ed. Cambridge, U.K.: Cambridge University Press, 1992, pp. 42-43.

[12] G. Mur, "Absorbing boundary conditions for the finite-difference approximation of the time-domain electromagnetic field equations, " IEEE Trans. Electromagnetic Compatibility, vol.EMC-23, pp.377-382, Nov. 1981.

[13] J. P. Berenger, "A perfect matched layer for the absorption of electromagnetic waves," J. Computational Physics, vol. 114, pp. 185-200, 1994.

[14] G. Liu and S. D. Gedney, "Perfectly matched layer media for an unconditionally stable three-dimensional ADI-FDTD method," IEEE Microwave and Guided Wave Letters, vol. 10, no. 7, pp. 261-263, July 2000.

[15] A. Zhu, S. Gedney, G. Liu, and J. A. Roden, "A novel perfect matched layer method for an unconditionally stable ADI-FDTD method," in IEEE AP-S Digest, vol. 4, pp.146-149 July 2001.

[16] T. W. Lee and S. Hagness, "Wave source conditions for the unconditionally stable ADI-FDTD method," in IEEE AP-S Digest, vol. 4, pp.142-145 July 2001.

[17] T. Namiki and K.Ito, "Numerical simulation of microstrip resonators and filters using the ADI-FDTD method," IEEE Trans. Microwave Theory Tech., vol. MTT-49, no. 4, pp. 665-670, Apr. 2001.

[18] T. Namiki and K.Ito, "Numerical simulation using ADI-FDTD method to estimate shielding effectiveness of thin conductive enclosures," IEEE Trans. Microwave Theory Tech., vol. MTT-49, no. 6, pp. 1060-1066, June 2001.